

Fabrication of NiO Nanowires/G Composite as Electrode Material for High Performance Supercapacitor

YuRong Ren¹, HengMa Wei¹, XiaoBing Huang², Bo Yang¹, JiaWei Wang¹, JianNing Ding^{1,*}

¹ School of Materials and Engineering, Changzhou University, Changzhou 213164, China

² College of Chemistry and Chemical Engineering, Hunan University of Arts and Science, Changde 415000, China

*E-mail: ryrchem@cczu.edu.cn

Received: 15 August 2014 / Accepted: 11 September 2014 / Published: 29 September 2014

Layer structure of graphene explores wide potential for the development of novel electrochemical materials. In this paper, NiO nanowires/G composite (NOG) was fabricated by synthesis of NiO nanowires (NWs) from nickel carbonates basic nanosheets anchored onto G sheets. NiO NWs were dispersed onto the surface of G sheets homogeneously. The layer structure of G sheets was maintained in NOG. The as-prepared composite is characterized using X-ray diffraction (XRD), Fourier transform infrared (FT-IR), Thermogravimetric analysis(TG), Transmission electron microscope(TEM), High Resolution Transmission Electron Microscopy(HRTEM) and X-ray photoelectron spectrum (XPS). NOG was employed as electrode active material for super capacitor. Excellent performances were obtained with high specific capacity up to 351 F g⁻¹ at current density of 2 A g⁻¹ in the initial cycle. A capacitance retention of 94.2 % can be maintained after 1000 cycles. With high charging-discharging current density up to 20 A g⁻¹, a high capacitor of 214.5 F g⁻¹ still can be achieved, suggesting its promising potential in supercapacitors. The improved structure stability and electron conductivity of NOG should be responsible for the capacitance properties.

Keywords: NiO nanowires, G sheets, Electrode material, Supercapacitor

1. INTRODUCTION

Supercapacitors with large power density and long lifespan are of great importance for their potential applications as energy storage devices in electric vehicles[1]. The nanostructure carbon materials have been researched substantially with very high rate performances and ultra stable

recyclability[2]. The energy storage of carbon materials is attributed to the formation of electric double layer[3]. The low specific capacitance of carbon materials as active matter is the main limited factor for their wide application as large energy density advices[4].

Pseudocapacitors work through the reduction-oxidation reaction occurred in electrode active matter and are able to be utilized with high energy and power density[5]. After all, the reduction-oxidation reaction provides very high theoretical capacitance for pseudocapacitor[6]. RuO_2 , MnO_2 , Co_3O_4 , nickel carbonate basic and NiO are typical electrode active matters for pseudocapacitors and have been investigated widely[7–11]. With the advantage of high capacitance, users of pseudocapacitors have to endure the associate disadvantage of, low conductivity, serious volume change and poor stability in the charging-discharging process[12]. These disadvantages are from the reduction-oxidation reaction in electrode active matters.

To overcome these disadvantages, an effective strategy is to prepare nanostructure electrode active materials to reduce the electrolyte ion diffusion pathway, enlarge the access area between active matter and electrolyte and improve the electron conductivity[13–15]. Single component nanostructure materials possess very high dispersive degree and limit their close attachment and connectivity in assembled electrode materials. The growth of nanostructure particles in charging-discharging process is another negative factor for the stability.

It is considered to be an ideal solution for these drawbacks in supercapacitor and pseudocapacitor to fabricate composite electrode active matters with carbon-based nano materials and metal oxide (hydroxide)-based nano materials[16–20]. The existence of carbon nanotubes, carbon fibers, graphite carbon layer and graphene sheets can form a conductive network to facilitate the electron transport[21–25]. The nanoscale inorganic particles provide short ion diffusion pathway and excellent ion diffusion properties are kept well. The chemical stability of carbon materials also buffer the volume change and protect the scale and structure of nanoparticles in the charging-discharging process. Following this design thought, various carbon-inorganic nanocomposite materials have been fabricated and investigated for ultracapacitors[25–29]. The reduced graphene oxide (G) as the most famous work plat for this synthesis strategy has been utilized to compose with many inorganic particles[30–35]. However, no inorganic particle with specific shape and morphology is used to compose with G sheets for high performance electrode active matter. Nanowires (NWs) with large ratio of length to diameter showed many unique properties in Li ion battery, fuel and solar cells. It should be believed that NWs may be an excellent alternative for the fabrication of composite materials with G sheets. NiO possessing high theoretical capacitance has chance to be composed with G sheets.

In this paper, NiO NWs/G (NOG) composite was designed and fabricated by synthesis of NiO NWs from nickel carbonate basic nanosheets anchored onto G sheets. NiO NWs were dispersed onto the surface of G sheets homogeneously. The layer structure of G sheets were well maintained in NOG. NOG was employed as electrode active material for supercapacitor. The superior performances including specific capacity, recycling stability and rate charging were obtained due to the high structural stability and electron conductivity of NOG.

2. EXPERIMENTAL SECTION

2.1 Preparation of material.

An aqueous suspension (10 mL water and 10 mL ethylene glycol) of GO (40 mg) was stirred for 10 min and then ultrasonicated for 2 h, followed by adding an aqueous solution (10 mL) of $\text{Ni}(\text{NO}_3)_2 \cdot 6\text{H}_2\text{O}$ (584 mg). The mixture was stirred for 3 h. Then, an aqueous solution (10 mL) of urea (240 mg) was added dropwise into above mixture with stirring for further 1 h. And then the mixture was transferred into autoclave heated to 180 °C and maintained at this temperature for 6 h. The resulted solid was collected and washed with deionized water and ethanol for three times, respectively and dried at 80 °C for 5 h. Then, the solid was heated to 300 °C with heating rate of 5 °C min^{-1} and kept for 2 h in Ar flow and NOG composite was obtained with a yield of 91.5 wt%. The synthesis procedure of pure NiO was the same as that for the NOG composite but without adding GO.

2.2 Characterization

Fourier transform infrared (FT-IR) spectra measurements were carried out on a Perkin Elmer Fourier transform infrared spectrophotometer. Raman spectrum was recorded on a Renishaw RM-2000 with excitation from the 514 nm line of an Ar-ion laser with a power of about 5 mW with a resolution of 1 cm^{-1} . The phase structure of as-prepared products were characterized with X-ray diffraction (XRD, Bruker D8 advance) with $\text{Cu K}\alpha$ $\lambda=1.5418$ Å).

X-ray photoelectron spectrum (XPS) were recorded on a 250XI X-ray photoelectron spectrometer with an Al $\text{K}\alpha$ and Mg/Al excitation source, where binding energies were calibrated by referencing the C1s peak (284.8 eV) to reduce the sample charge effect. The morphology of as-prepared products was studied by using transmission electron microscope (TEM, Hitachi H7650B, operating at 120 kV), and high resolution TEM (HRTEM, TECNAI G² 20 electron microscope, operating at 200 kV). TGA Q5000 V3.15 Build 263 instrument was used to performed the thermal analysis by heating under an air atmosphere to 850 °C at a rate of 10 °C min^{-1} .

To prepare the electrodes for supercapacitors, 80 wt% NOG active material, 10 wt% carbon black (Super P) and 10 wt% polytetrafluoroethylene (PTFE) binder were mixed together and pressed on nickel foam. For the electrochemical testing in an aqueous electrolyte, three-electrode test cells were assembled with a working electrode (a platinum foil with pasted mixture), a reference electrode (saturated calomel electrode, SCE), and a counter-electrode (a platinum foil). Aqueous solution (6 M) of KOH was used as the electrolyte. Cyclic voltammetry (CV) measurements were carried out in the potential range of 0-0.45 V (vs. Ag/AgCl) on an electrochemistry workstation (CHI660E). The galvanostatic charging-discharging measurements were performed on the electrochemistry workstation. The electrochemical impedance spectroscopy (EIS) measurements were performed over a frequency range from 10^5 to 10^{-2} Hz at the amplitude of the sinusoidal voltage of 5 mV and RT using the electrochemistry workstation. For comparison, the electrode of pure NiO is also prepared by the above synthesis method and tested appropriately.

For CV measurement, the specific capacitances at different scan rates were calculated by the following equation,

$$C_s = Q/(\Delta U * m) = \frac{1}{\Delta U * m} \int i dt$$

where C_s is the specific discharge capacitance in F/g, i is the current in A, t is the discharge time in s, ΔU is potential window in V, and m is the mass of NOG in electrode.

For galvanostatic charging-discharging measurement, the specific capacitances at different current densities were calculated by the following equation,

$$C_s = (i * \Delta t) / (\Delta U)$$

where C_s is the specific discharge capacitance in $F g^{-1}$, i is the current density in $A g^{-1}$, Δt is the discharge time in s, ΔU is potential drop during discharge in V.

3. RESULTS AND DISCUSSION

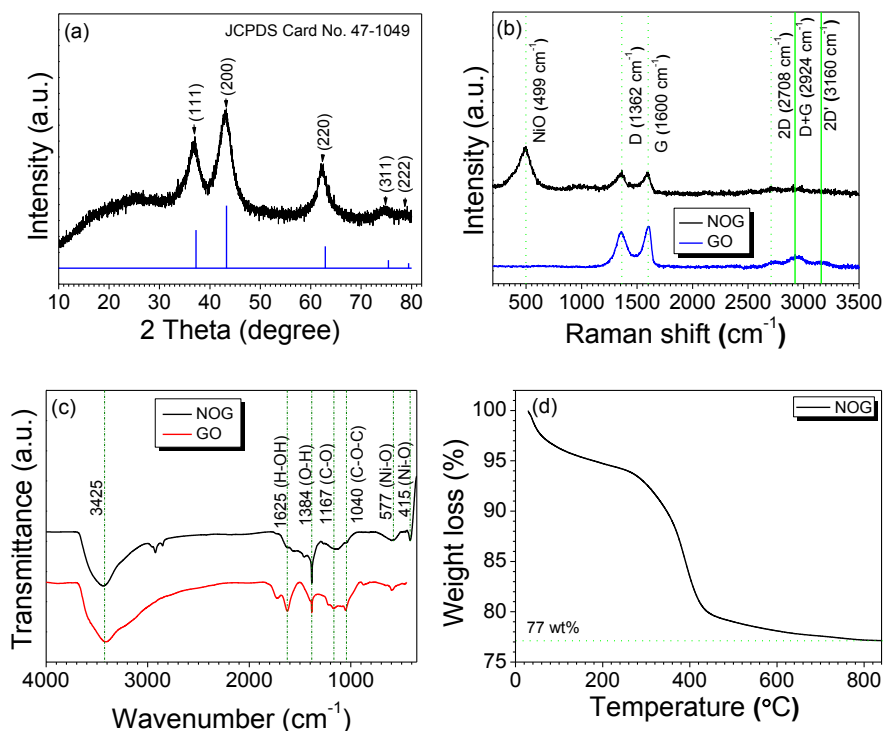


Figure 1. (a) XRD pattern of NOG, (b) Raman spectra of GO and NOG, (c) FTIR spectra of GO and NOG and (d) TG curve of NOG.

The phase and structure information of composite was measured by X-ray diffraction pattern (Figure 1a). No clear peak can be found at 12.9° , which shows that GO have been reduced completely to G sheets[31]. The very weak wide diffraction peak round 24.0° evidences that the G sheets possess high disperse degree in the composite without aggregate G sheets formed. The diffraction peaks at 36.8 (111), 43.2 (200), 62.3 (220), 74.8 (311) and 78.6 (222) are agree in the standard pattern of cubic phase NiO (JCPDS No. 47–1049). The NiO possesses space group of Fm-3m and cell parameters:

$a=b=c=4.177 \text{ \AA}$, $\alpha=\beta=\gamma=90^\circ$. [32] The precursor was evidenced as nickel carbonate basic by XRD pattern (Figure S1).

Raman spectra provide further information of NOG (Figure 1b). The Raman shift at 499 cm^{-1} corresponds to the characteristic of NiO. The peaks at 1362 and 1600 cm^{-1} should be attributed to D and G mode vibration of G sheets, respectively [33]. The D peak of NOG increased compared to that of pristine GO. The composite interaction between NiO NWs and G sheets induced the ordered degree of carbon atoms in G sheets decrease. [34] The decreasing G peak corresponding to the graphite domains in G sheets also provides further evidence for the interaction in composite material. The wide and overlapped 2D (2708 cm^{-1}), D+G (2924 cm^{-1}) and 2D' (3160 cm^{-1}) peaks show that the GO sheets possess multi-layer structures [35].

Fourier transform infrared (FTIR) spectra give some information of functional groups in composite materials (Figure 1c). The peak at 1625 cm^{-1} existed in the spectra of GO and composite should be attributed to the stretching vibration of adsorbed water [36]. The peak at 1167 cm^{-1} is from the hydroxyl C-O bond in the G sheets. The peak at 1040 cm^{-1} is from the epoxide C-O-C bond in the G sheets. The peak at 415 and 577 cm^{-1} is corresponding to the framework stretching vibration of NiO [37]. The disappearance of peak at 1730 cm^{-1} showed the entire reduction of GO to G in the NOG. For the TG curve of NOG (Figure 1d), a large weight loss occurred at about $300\text{--}600^\circ\text{C}$, which is ascribed to the decomposition and oxidation of G sheets. Therefore the weight percentage of G and NiO NWs in NOG could be determined to be $\sim 23 \text{ wt\%}$ and 77 wt\% , respectively.

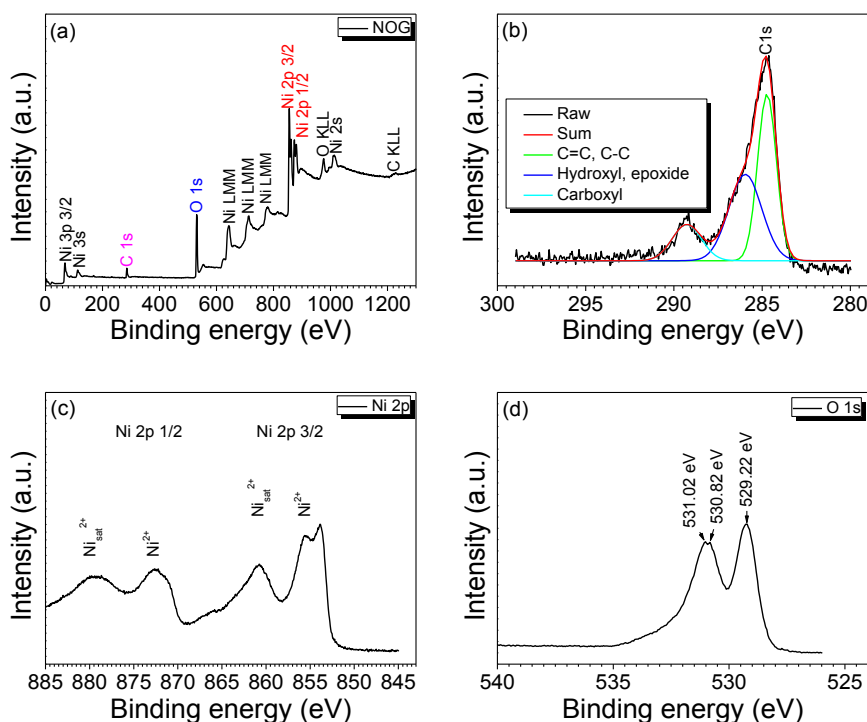


Figure 2. (a) XPS survey spectra of NOG and fine spectra of (b) C1s, (c) Ni2p and (d) O1s.

X-ray photoelectron spectra (XPS) were used to investigate the chemical state of elements in NOG. In the survey spectrum, the peaks of C1s, Ni2p and O1s electrons can be observed clearly, which display that the main composition of NOG includes C, Ni and O elements (Figure 2a). In the fine structure of C1s spectrum treated by multi peaks fitting, the main peak at 284.8 eV is attributed to carbon atoms in graphene domains of from G sheets (Figure 2b) [38]. The secondary peak at 286.6 eV corresponds to the carbon atoms connecting to hydroxyl and epoxide. The low peak at 287.1 eV is induced by carbon atoms in carbonyl of ketone, which were reduced in NOG composite after reduction process. The binding energy peaks at 779.21 and 793.99 eV corresponding to Ni²⁺ atoms in NiO NWs are consistent to other characterization results[39]. In the fine spectra of O1s, the peak at 529.22 eV should be due to the oxygen atoms in NiO NWs and the two peaks at 530.82 and 531.02 eV should be due to the oxygen atoms in the oxygen containing functional groups of G sheets[40].

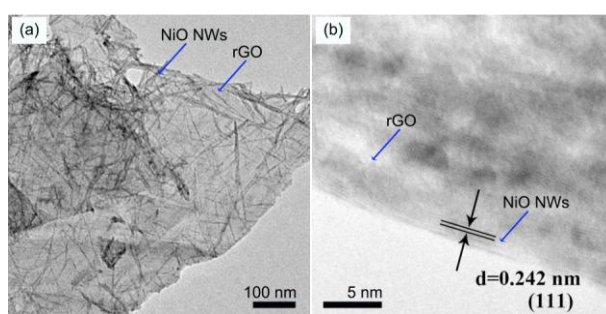


Figure 3. (a) TEM and (b) HRTEM images of NOG.

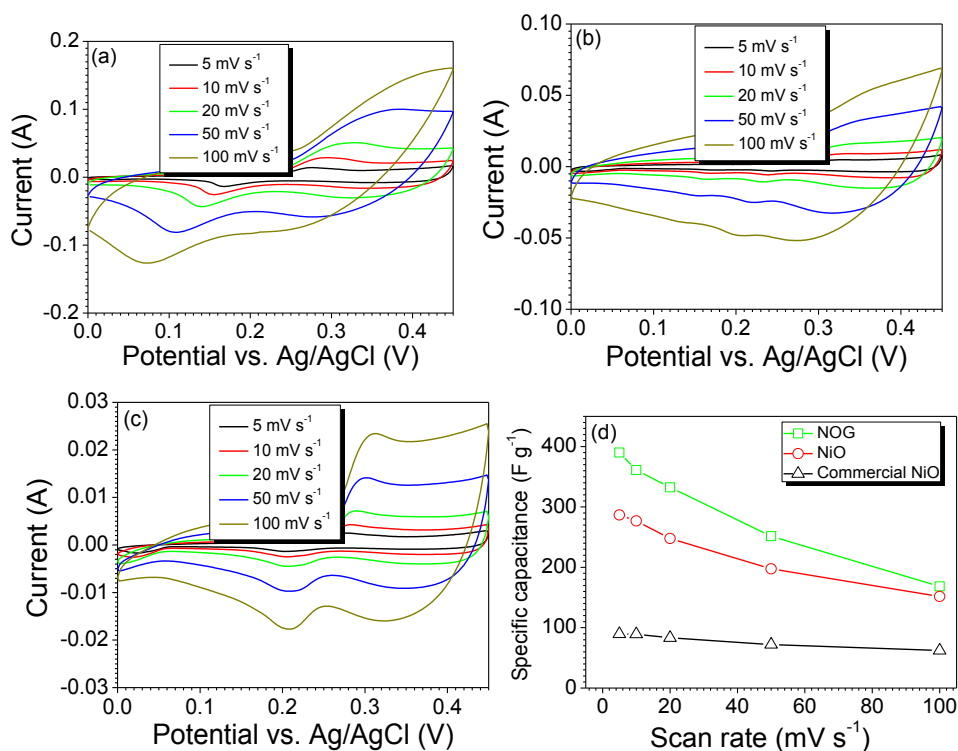


Figure 4. CV curves of (a) NOG, (b) pure NiO, (c) commercial NiO; and (d) specific capacitance-scan rate plot for NOG, NiO and commercial NiO with CV measurement.

The micro structure of NOG was observed in TEM and HRTEM images (Figure 3). The G sheet remains well as layer structure. The NiO NWs lied homogeneously on the surface of G sheets (Figure 3a, b). The diameter distribution of NiO NWs is uniformly concentrated in the range of 5-10 nm and the length is concentrated in the range of 50-100 nm (Figure 3a). After ultrasonic treatment, the NiO NWs still are paved on the surface of G sheets and no isolate NiO NWs were observed out of the G sheets. The composite structure ensures the stability of NOG in the utility process. The lattice space of 0.242 nm is attributed to the crystalline plane (111) of NiO and provides a further evidence for the existence of NiO NWs in NOG (Figure 3c, d) [41].

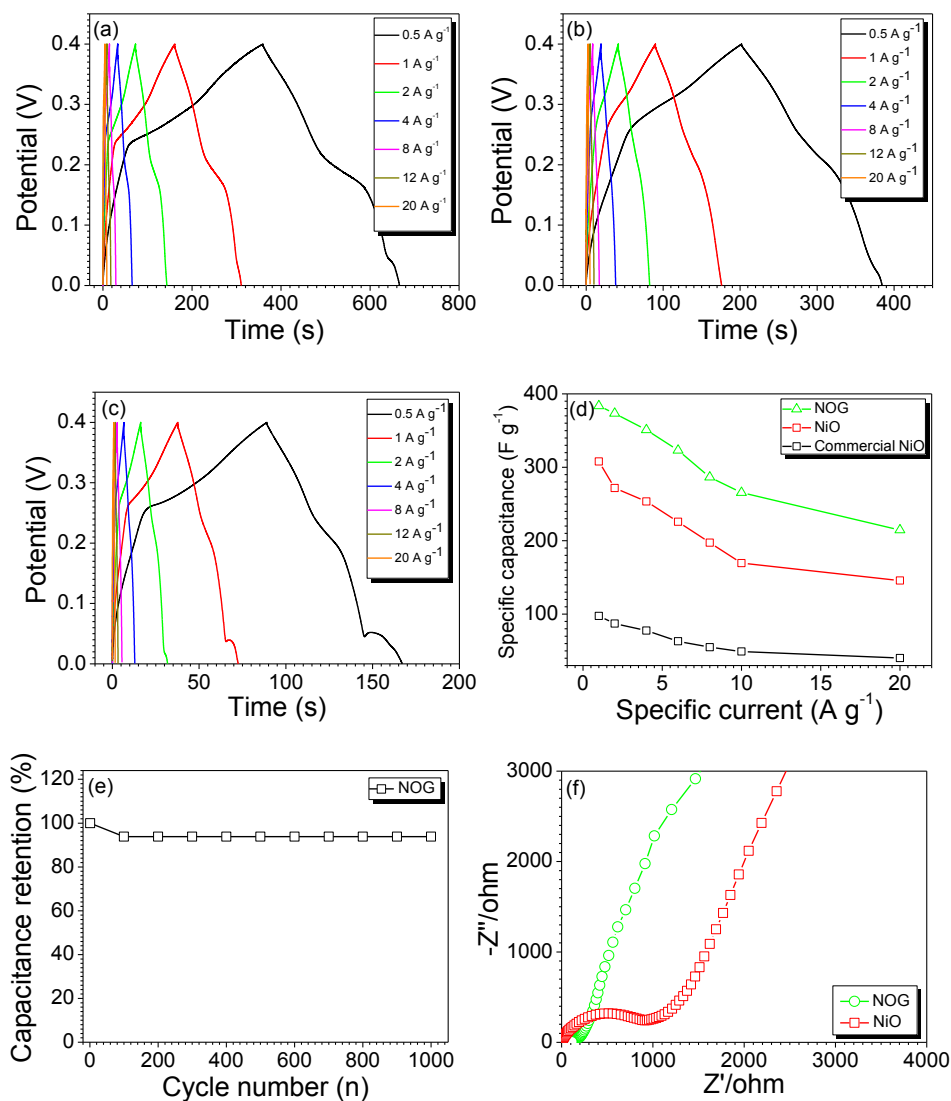


Figure 5. Potential-time plots of (a) NOG, (b) pure NiO, (c) commercial NiO; (d) specific capacity-current density plot for NOG, NiO and commercial NiO, (e) capacitance retention of NOG with galvanostatic charging-discharging measurement and (f) Nyquist plots for NOG and NiO before cycle.

In the CV curve of NOG at various scan rates in the potential range of 0-0.45 V vs Ag/AgCl, a pair of oxidation and reduction peaks can be observed (Figure 4a) and should be due to the reversible

reaction of $\text{NiO} + \text{OH}^- \leftrightarrow \text{NiOOH} + \text{e}^-$ [42]. With increasing scan rate, the oxidation peak shifted to a more positive potential and the reduction peak shifted to a more negative potential, correspondingly, the increased current was obtained. This tendency suggests that the internal diffusion resistance increase with increased scan rate [43]. The gravimetric capacitance of NOG with various scan rates were calculated and compared to those of NiO and commercial NiO (Figure 4b and 4c). The gravimetric capacitance reached 390.1, 360.1, 333.3, 251.7 and 168.3 F g^{-1} at 5, 10, 20, 50 and 100 mV s^{-1} . These gravimetric capacitance of NOG are significantly higher than those of NiO and commercial NiO with the same scan rates (Figure 4d).

The galvanostatic charging-discharging processes with various current densities were used to investigate the potential window (Figure 5a). The charging potential is in the range of 0.25-0.40 V, and the discharging potential is in the range of 0.35-0.05 V, which is consistent with the oxidation-reduction peaks in CV curves. The gravimetric capacitance of NOG with various current densities were calculated and compared to those of NiO and commercial NiO (Figure 5d). The gravimetric capacitance reached 383.5, 373.5, 351.0, 323.0, 286.6, 265.5 and 214.5 F g^{-1} with current densities of 0.5, 1, 2, 4, 8, 12 and 20 mA g^{-1} , which are similar to those capacitances calculated from CV curves (Figure 5b and 5c). From the current densities of 0.5, 1, 2, 4, 8, 12 and 20 mA g^{-1} , the retention ratio of gravimetric capacitances are 100, 97.4, 91.5, 84.2, 74.7, 69.2 and 55.9%. These rate performances suggest that superior electron transport and efficient ion diffusion to the surface of active matter were carried out in NOG [44]. These gravimetric capacitances are higher than those of NiO and commercial NiO.

The recycling stability of NOG was evaluated in a long-term galvanostatic charging-discharging process (Figure 5e). The specific capacitance kept constant value from the second cycle in the last 1000 cycles. The capacitance retention of 94% was achieved at a current density of 2 A g^{-1} . The electrochemical impedance spectra (EIS) displayed a small half cycle curves and larger slope of the straight line for NOG compared to those for NiO before cycles (Figure 5f, S4). In the Nyquist plots of the NOG electrode, the almost vertical line in the low frequency region indicates a good capacitive behavior [45]. In the high frequency region, the NOG electrode has an equivalent series resistance (ESR) of about 178.6 ohm, suggesting a low electrode resistance and high charge-transfer rate between the electrolyte and the active matter [46]. This characterization should be derived from the improved electron and ion conductivity of NOG [47]. The existence of G sheets is benefit to the electron and ion conductivity into NOG composite [48]. The NiO NWs improved the accessibility of NOG. The assembly between G sheets and NiO NWs formed porous structure also facilitate the penetration of electrolyte into electrode matter [49]. These factors are responsible for the superior electrochemical properties of NOG.

4. CONCLUSIONS

In conclusion, NOG had been fabricated by synthesis of NWs from nickel carbonate and G sheets. NiO NWs with average diameter of 5-10 nm and length of 50-100 nm were anchored onto the

surface of G sheets homogeneously, and the layer structure of G sheets also were maintained in NOG. With NOG as electrode active material for supercapacitor, excellent performances were obtained. The electrode comprises high specific capacity up to 351 F g^{-1} at current density of 2 A g^{-1} in the initial cycle and capacitance retention of 94.2 % after 1000 cycles. With high rate up to 20 A g^{-1} , a high capacitor of 214.5 F g^{-1} still can be achieved. The assemble and interation between layer structure of G sheets and nanoscale of NiO NWs warranted high structure stability and accessibility of NOG. The improved structure stability and electron conductivity of NOG should be responsible for the capacitance properties. This NOG composite material and synthesis method will find potential application for design of supercapacitor and novel functional materials.

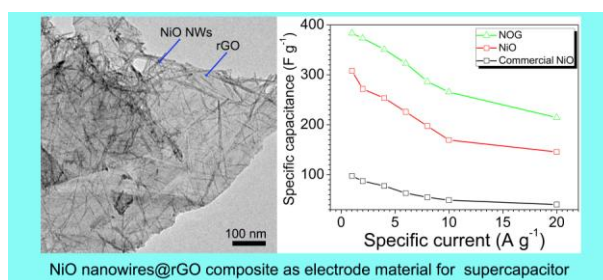
ACKNOWLEDGEMENT

Financial support from the National Natural Science Foundation of China (51342010 and 5134077), Science and Technology Department of Science and Technology Project in Jiangsu Province (BY2014037-31) are acknowledged, Hunan Provincial Natural Science Foundation of China (13JJ4100 and 12JJ8004).

References

1. K.Naoi, S.Ishimoto, J. Miyamoto, W. Naoi, *Energy Environ. Sci.*, 5(2012)9363–9373.
2. S. Lee, V. Sridhar, J. Jung, K. Karthikeyan, Y. Lee, R. Mukherjee; N. Koratkar, I. Oh, *ACS Nano*, 7(2013)4242–4251.
3. A. Elsen, B. Murphy, B. Ocko, L. Tamam, M. Deutsch, I. Kuzmenko, O. Magnussen, *Phys. Rev. Lett.*, 104(2010)105501.
4. G.Eda, M.Chhowalla, *Nano Lett.*, 9(2009)814–818.
5. P. Simon, Y. Gogotsi, *Nature Mater.*, 7(2008)845–854.
6. J. Miller, P.Simon, *Science*, 321(2008) 651–652.
7. J. Zang, S. Bao, C. M.Li, H. Bian, X. Cui, Q. Bao, C. Sun, J.Guo, K. Lian, *Phys. Chem. C*, 112(2008)14843–14847.
8. G. Yu, L. Hu, N. Liu, H. Wang, M. Vosgueritchian, Y. Yang, Y. Cui, Z. Bao, *Nano Lett.*, 11(2011)4438–4442.
9. X. Xia, J. Tu, Y. Mai, X.Wang, C. Gu, X. Zhao, *J. Mater. Chem.*, 21(2011)9319–9325.
10. H. Wang, H. Casalongue, Y. Liang, H. Dai, *J. Am. Chem. Soc.*, 132(2010)7472–7477.
11. B. Zhao, J. Song, P. Liu, W. Xu, T. Fang, Z.Jiao, H. Zhang, Y. Jiang, *J. Mater. Chem.*, 21(2011)18792–18798.
12. M.Toupin, T.Brousse, D. Be' langer, *Chem. Mater.*, 14(2002) 3946–3952.
13. Y.Si, E.Samulski, *Chem. Mater.*, 20(2008)6792–6797.
14. L.Zhang, R.Zhou, X.Zhao, *J. Mater. Chem.*, 20(2010)5983–5992.
15. H. Wang, J.Robinson, G.Diankov, H. Dai, *J. Am. Chem. Soc.*, 132(2010)3270–3271.
16. M. Kaempgen, J.Ma, Y.Cui, G.Gruner, *Nano Lett.*, 9(2009) 1872–1876.
17. S.Chen, J.Zhu, X. Wu, Q. Han, X.Wang, *ACS Nano*, 4(2010)2822–2830.
18. D.Wang, F.Li, M.Liu, G.Lu, H. Cheng, *Angew. Chem.*, 120(2008) 379–382.
19. J. Lee, K. Smith, C. Hayner, H. Kung, *Chem. Commun.*, 46(2010)2025–2027.
20. M. Hantel, T.Kaspar, R.Nesper, A.Wokaun, R. Kötz, *Electrochem. Commun.*, 13(2011)90–92.
21. C.Yuan, S.Xiong, X. Zhang, L. Shen, Z F.hang, B. Gao, L.Su, *Nano Res.*, 2(2009)722–732.
22. W.Lv, F.Sun, D. Tang, H. Fang, C.Liu, Q. Yang, H. Cheng, *J. Mater. Chem.*, 21(2011) 9014–9019.

23. C.Yuan, B.Gao, L. Shen, S. Yang, L. Hao, X. Lu, F. Zhang, L. Zhang, X.Zhang, *Nanoscale*, 3(2011)529–545.
24. C.Yuan, X. Zhang, L.Hou, L.Shen, D.Li, F.Zhang, C. Fan, J.Li, *J. Mater. Chem.*, 20(2010)10809–10816.
25. J.Yan, T.Wei, B.Shao, F.Ma, Z. Fan, M. Zhang, C.Zheng, Y. Shang, W. Qian, F. Wei, *Carbon*, 48(2010)1731–1737.
26. D.Pech, M.Brunet, H.Durou, P.Huang, V.Mochalin, Y.Gogotsi, P.Taberna, P.Simon, *Nature Nanotech.*, 5(2010)651–654.
27. S. Lee, J.Kim, S.Chen, P. Hammond, S Y.hao-Horn, *ACS Nano*, 4(2010)3889–3896.
28. P.Simon, Y.Gogotsi, *Phil. Trans. R. Soc. A*, 368(2010) 3457–3767.
29. X. Lang, A.Hirata, T. Fujita, M. Chen, *Nature Nanotech.*, 6(2011) 232–236.
30. Q.Chen, Y. Meng, C. Hu, Y.Zhao, H.Shao, N.Chen, L.Qu, *J. Power Sources*, 247(2014) 32–39.
31. B. Li, H. Cao, J.Shao, M.Qu, *Chem. Commun.*, 47(2011)10374–10376.
32. F. Luan, G. Wang, Y. Ling, X. Lu, H. Wang, Y. Tong, X. Liu, Y. Li, *Nanoscale*, 5(2013) 7984–7990.
33. J. Johns, J.Alaboson, S.Patwardhan, C. Ryder, G.Schatz, M. Hersam, *J. Am. Chem. Soc.*, 135(2013)18121–18125.
34. J. An, S.Park, O.Kwon, J. Bae, J. Jang, *ACS Nano*, 7(2013) 10563–10571.
35. W.Li, F.Wang, S. Feng, J.Wang, Z.Sun, B.Li, Y.Li, J.Yang, A. Elzatahry, Y.Xia, D.Zhao, *J. Am. Chem. Soc.*, 135(2013) 18300–18303.
36. H. Cao, B. Li, J. Zhang, F. Lian, X. Kong, M. Qu, *J. Mater. Chem.*, 22(2012)9759–9766.
37. D.Xie, Q.Su, W.Yuan, Z. Dong, J.Zhang, G.Du, *J. Phys. Chem. C*, 117(2013) 24121–24128.
38. B. Li, H.Cao, J. Zhang, M. Qu, L. Fang, X. Kong, *J. Mater. Chem.*, 22(2012)2851–2854.
39. L.Zhuo, Y.Wu, Z.Wei, L.Wang, Y.Yu, X.Zhang, F.Zhao, *ACS Appl. Mater. Interfaces*, 5(2013)7065–7071.
40. V.Dao, L. Larina, K.Jung, J.Lee, H.Choi, *Nanoscale*, 6(2013)477–82.
41. B. Qu, L.Hu, Y.Chen, C.Li, Q.Li, Y.Wang, W. Wei, L.Chen, T.Wang, *J. Mater. Chem. A*, 1(2013)7023–7026.
42. W.Li, Y. Bu, H. Jin, *Energy & Fuels*, 27(2013) 6304–6310.
43. K.Hercule, Q.Wei, A. Khan, Y.Zhao, X.Tian, L.Mai, *Nano Lett.*, 13(2013) 5685–5691.
44. L.Huang, D. Chen, Y.Ding, S.Feng, Z.Wang, M.Liu, *Nano Lett.*, 13(2013) 3135–3139.
45. J.Lee, A.Hall, J. Kim, T.Mallouk, *Chem. Mater.*, 24(2012) 1158–1164.
46. A. Vu, X.Li, Phillips, A.Han, W.Smyrl, P.Buhlmann, A.Stein, *Chem. Mater.*, 25(2013)4137–4148.
47. J. Luo, H. Jang, J. Huang, *ACS nano*, 7(2013)1464–1471.
48. J.Lee, N.Park, B.Kim, J D.ung, K.Im, J.Hur, J.Choi, *ACS nano*, 7(2013)9366–9374.
49. V. Le, H.Kim, A.Ghosh, J.Kim, J.Chang, Q. Vu, D. Pham, J. Lee, S. Kim, Y. Lee, *ACS nano*, 7(2013)5940–5947.



NiO nanowires/G composite (NOG) was fabricated by synthesis of NiO nanowires (NWs) anchored homogeneously onto G sheets. NOG was employed as electrode active material for supercapacitor. Excellent performances were obtained with high specific capacity up to 351 F g^{-1} at current density of 2 A g^{-1} in the initial cycle and capacitance retention of 94.2 % after 1000 cycles. The improved

structure stability and electron conductivity of NOG should be responsible for the capacitance properties.

© 2014 The Authors. Published by ESG (www.electrochemsci.org). This article is an open access article distributed under the terms and conditions of the Creative Commons Attribution license (<http://creativecommons.org/licenses/by/4.0/>).